Article

Improvement in the Hydrogen Storage Properties of MgH2 by Adding NaAlH4

Young Jun Kwak , Myoung Youp Song * , Ki-Tae Lee

Posted Date: 3 January 2024

doi: 10.20944/preprints202401.0201.v1

Keywords: hydrogen storage; MgH2; NaAlH4; decomposition temperature; hydrogen absorption; release rates

Article

Improvement in the Hydrogen Storage Properties of MgH_2 by adding $NaAlH_4$

Young Jun Kwak [1,2], Myoung Youp Song [1,2,*] and Ki-Tae Lee [1,2,3]

[1] Division of Advanced Materials Engineering, Jeonbuk National University, 567 Baekje-daero Deokjin-gu Jeonju, 54896, Republic of Korea
[2] Hydrogen & Fuel Cell Research Center, Engineering Research Institute, Jeonbuk National University, 567 Baekje-daero Deokjin-gu Jeonju, 54896, Republic of Korea
[3] Department of Energy Storage/Conversion Engineering of Graduate School (BK21 FOUR), Jeonbuk National University, 567 Baekje-daero Deokjin-gu Jeonju, 54896, Republic of Korea
* Correspondence: songmy@jbnu.ac.kr (M. Y. Song); Tel.: +82-10-3260-2379

Abstract: Milled MgH_2, $NaAlH_4$, MgH_2–10$NaAlH_4$, MgH_2–30$NaAlH_4$, MgH_2–50$NaAlH_4$, and MgH_2–2Ni-10$NaAlH_4$ samples were prepared by milling in hydrogen atmosphere (reactive mechanical milling, RMM). Decomposition temperatures of milled MgH_2, $NaAlH_4$, MgH_2–10$NaAlH_4$, and MgH_2–30$NaAlH_4$ were examined in a Sieverts-type hydrogen-absorption and release apparatus, in which the hydrogen pressures were kept constant during hydrogen absorption or release. As the content of $NaAlH_4$ in the sample increased, the temperature at the highest peak in the ratio of increase in H_r to increase in T, dH_r/dT, versus T curve decreased. The higher content of $NaAlH_4$ is believed to have made effects of reactive mechanical milling stronger. Effects of the $NaAlH_4$ content on the temperatures of intermediate reactions were studied for MgH_2 – $NaAlH_4$ composites. Phase formation in the cycled MgH_2–50$NaAlH_4$ were investigated. The hydrogen-storage properties of MgH_2–30$NaAlH_4$ were compared with those of Mg-based alloys in which oxide, halides, or fluoride was added.

Keywords: hydrogen storage; MgH_2; $NaAlH_4$; decomposition temperature; hydrogen absorption and release rates

1. Introduction

Clean alternative energies have drawn interest to prevent air pollution and climate change. One of the clean alternative energies is hydrogen energy, which is the energy produced by the reaction of hydrogen with oxygen, producing water as a by-product. The problems to be solved for applying the hydrogen energy to practical use are hydrogen production and storage. One of the methods to store hydrogen is using metal hydrides. We are interested in synthesizing Mg-based hydrides with high reaction rates and high hydrogen storage capacities.

Many works were performed to improve the hydriding and dehydriding kinetics of Mg [1–6]. Researchers were interested in improving the hydrogen storage properties of MgH_2 by adding $NaAlH_4$ with a high hydrogen-storage capacity [7–11]. Ali and Ismail [7] reviewed the hydrogen storage properties of the Mg–Na–Al system. The complex hydride $NaAlH_4$ releases hydrogen via three step reactions:

At 458 – 503 K, $3NaAlH_4 \rightarrow Na_3AlH_6 + 2Al + 3H_2$ (1)

At 533 K, $Na_3AlH_6 \rightarrow 3NaH + Al + \frac{1}{2}H_2$ (2)

At 708 K, $3NaH \rightarrow 3Na + (3/2)H_2$. (3)

Ali and Ismail [7] reported that addition of NaAlH4 could destabilize the MgH2 effectively and the hydrogen storage properties of NaAlH4 has could also be improved by adding MgH_2. The MgH_2–$NaAlH_4$ system exhibited much better dehydriding properties than unary MgH_2 and $NaAlH_4$.

 doi:10.20944/preprints202401.0201.v1

Ismail et al. [10] reported that the following reaction takes place within the temperature range from 443 to 485 K:

$$NaAlH_4 + MgH_2 \rightarrow NaMgH_3 + Al + 1.5H_2 \quad (4)$$

A mixing decomposition of (4) the reaction of MgH_2 with Al and (5) the decomposition of the excessive MgH_2 occurs reversibly between 553 K and 603 K [10].

$$17MgH_2 + 12Al \Leftrightarrow Mg_{17}Al_{12} + 17H_2 \quad (5)$$

$$MgH_2 \Leftrightarrow Mg + H_2 \quad (6)$$

They also reported that $NaMgH_3$ decomposes between 603 K and 633 K by the following reversible reaction:

$$NaMgH_3 \Leftrightarrow NaH + Mg + H_2 \quad (7)$$

NaH decomposes between 633 K and 648 K by the following reversible reaction [10]:

$$NaH \Leftrightarrow Na + (1/2)H_2. \quad (8)$$

In this work, milled MgH_2, $NaAlH_4$, MgH_2–$10NaAlH_4$ (with a composition of 90 wt% MgH_2 + 10 wt% $NaAlH_4$), MgH_2–$30NaAlH_4$ (70 wt% MgH_2 + 30 wt% $NaAlH_4$), MgH_2–$50NaAlH_4$ (50 wt% MgH_2 + 50 wt% $NaAlH_4$), and MgH_2–$2Ni$-$10NaAlH_4$ (88 wt% MgH_2 + 2 wt% Ni + 10wt% $NaAlH_4$) samples were prepared by milling in hydrogen atmosphere (reactive mechanical milling, RMM). Decomposition temperatures of milled MgH_2, $NaAlH_4$, MgH_2–$10NaAlH_4$, and MgH_2–$30NaAlH_4$ were examined heating at a rate of 5 ~ 6 K in a Sieverts-type hydrogen-absorption and release apparatus and phase formation in cycled MgH_2–$50NaAlH_4$ were investigated.

2. Experimental Procedures

As starting materials, were used MgH_2 (magnesium hydride, purity 98%, Alfa Aesar), $NaAlH_4$ (Hydrogen-storage grade, Aldrich), and Ni (average particle size 2.2–3.0 μm, purity 99.9 % metal basis, C typically < 0.1%, Alfa Aesar).

Reactive mechanical milling (RMM) was carried out in a planetary ball mill (Planetary Mono Mill; Pulverisette 6, Fritsch). A mixture with the planned composition (total weight = 8 g) was mixed in a stainless-steel container (with 105 hardened steel balls, total weight = 360 g) sealed hermetically, the sample to ball weight ratio being 1/45. All samples were handled in a glove box in argon atmosphere. The disc revolution speed was 400 rpm. The mill container (volume of 250 ml) was then filled with high purity hydrogen gas of about 12 bar. The RMM was performed for 6 h (by repeating milling for 15 min and pause for 5 min 24 times). Hydrogen was refilled every 2 h milling (every eight milling times).

The absorbed or released hydrogen quantity was measured as a function of time by a volumetric method, using Siverts-type hydrogen-absorption and release apparatus previously described [21]. The hydrogen pressure in the reactor was kept as 12 bar during hydriding by dosing the quantity of hydrogen absorbed from a reservoir of known volume. The hydrogen pressure in the reactor was kept as 1.0 bar during dehydriding by removing the quantity of hydrogen released from the reactor to a reservoir of known volume. 0.5 g of the samples was used for these measurements. Samples after hydrogen absorption-release cycling were characterized by X-ray diffraction (XRD) with Cu Ka radiation, using a Bruker D8 Advance (Karlsruhe, Germany) powder diffractometer.

3. Results

The quantity of released hydrogen, H_r (wt% H), was calculated using the sample weight as a standard.

Figure 1 shows quantity of released hydrogen (H_r) versus temperature T curves and the ratio of increase in H_r to increase in T, dH_r/dT, versus T curves for milled MgH_2, MgH_2-$10NaAlH_4$, MgH_2-$30NaAlH_4$, and $NaAlH_4$ samples. The samples were heated at a heating rate of 5 ~ 6 K in 1.0 bar hydrogen. Table 1 presents the temperatures (K) at peaks in the dH_r/dT versus T curves for milled MgH_2, MgH_2-$10NaAlH_4$, MgH_2-$30NaAlH_4$, and NaAlH4 samples. The highest peaks appear at 638, 600, 592, and 455 K, respectively, for milled MgH_2, MgH_2-$10NaAlH_4$, MgH_2-$30NaAlH_4$, and $NaAlH_4$.

Preprints (www.preprints.org) | NOT PEER-REVIEWED | Posted: 3 January 2024 doi:10.20944/preprints202401.0201.v1

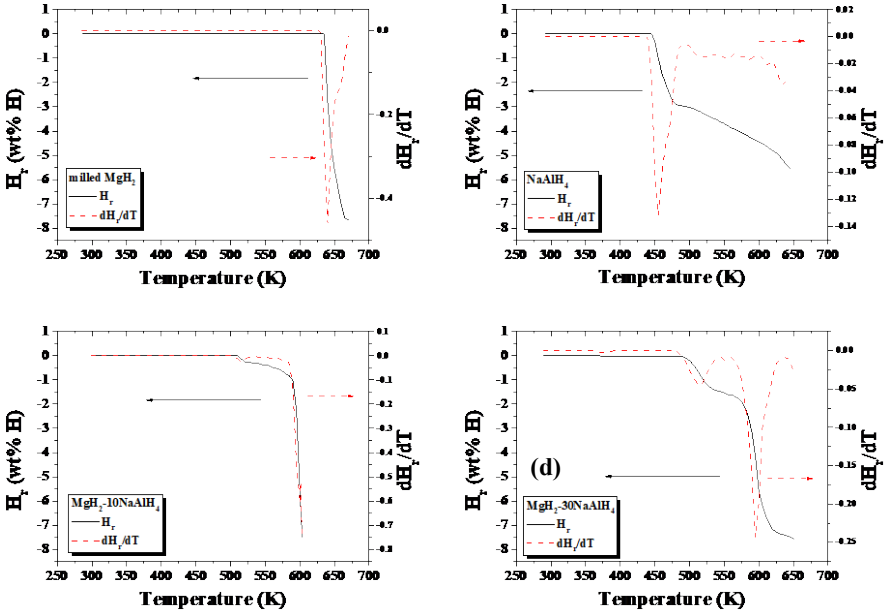

Figure 1. Quantity of released hydrogen (H_r) versus temperature T curves and dH_r/dT versus T curves for milled MgH_2, MgH_2-10$NaAlH_4$, MgH_2-30$NaAlH_4$, and $NaAlH_4$ samples. The samples were heated at a heating rate of 5 ~ 6 K in 1.0 bar hydrogen.

Table 1. Temperatures (K) at peaks in the dH_r/dT versus T curves for milled MgH_2, MgH_2-10$NaAlH_4$, MgH_2-30$NaAlH_4$, and $NaAlH_4$ samples.

	Peak	Highest Peak	Peak	Peak
milled MgH_2		638		
MgH_2-10$NaAlH_4$	513	600		
MgH_2-30$NaAlH_4$	512	592		
$NaAlH_4$		455	552	631

Figure 2 shows the quantity of released hydrogen (H_r) versus temperature curves for milled MgH_2, MgH_2-10$NaAlH_4$, MgH_2-30$NaAlH_4$, and $NaAlH_4$ samples. The samples were heated at a heating rate of 5 ~ 6 K in 1.0 bar hydrogen. The points were marked so that they correspond to the beginning and ending points of the peaks in Figure 1. Table 2 presents the temperatures (K) at the marked points in the H_r versus T curves for milled MgH_2, MgH_2-10$NaAlH_4$, MgH_2-30$NaAlH_4$, and $NaAlH_4$ samples.

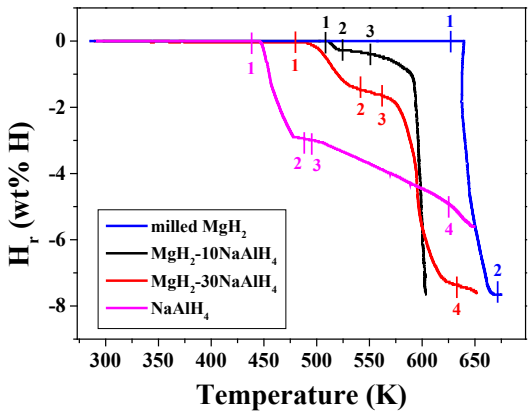

Preprints (www.preprints.org) | NOT PEER-REVIEWED | Posted: 3 January 2024 doi:10.20944/preprints202401.0201.v1

Figure 2. Quantity of released hydrogen (H_r) versus temperature T curves for milled MgH_2, MgH_2-10$NaAlH_4$, MgH_2-30$NaAlH_4$, and $NaAlH_4$ samples. The samples were heated at a heating rate of 5 ~ 6 K in 1.0 bar hydrogen.

Table 2. Temperatures (K) at the marked points in the H_r versus T curves for milled MgH_2, MgH_2-10$NaAlH_4$, MgH_2-30$NaAlH_4$, and $NaAlH_4$ samples.

Marked Points	1	2	3	4
milled MgH_2	627	673		
MgH_2-10$NaAlH_4$	508	525	550	
MgH_2-30$NaAlH_4$	480	541	562	633
$NaAlH_4$	438	488	495	625

Hydrogen release begins at 627 K for the as-milled MgH_2. Hydrogen release from the $NaAlH_4$ begins at 438 K and the slope of the H_r versus temperature curve then changes at 488, 495, and 625 K. MgH_2-10$NaAlH_4$ begins to release hydrogen at 508 K and slopes of the H_r versus temperature curves change at 525 K and 550 K. MgH_2-30$NaAlH_4$ begins to release hydrogen at 480 K and slopes of the H_r versus temperature curves change at 541, 562, and 633 K.

As the content of $NaAlH_4$ in the sample increases, the temperature at the highest peak decreases. The higher content of $NaAlH_4$ is believed to have made effects of reactive mechanical grinding stronger, lowering the temperatures for the reaction. The effects of reactive mechanical grinding are thought to be creation of defects, making cracks and clean surfaces, and decreasing particle sizes.

The XRD pattern of MgH_2-50$NaAlH_4$ dehydrided after number of cycles, n, of 4 at 593 K is shown in Figure 3. The sample contains Al, MgO, Al_3Mg_2, MgH_2, and $Mg_{17}Al_{12}$. Even though the sample was dehydrided, a small amount of MgH_2 remains. Al, formed from the reactions (4), is believed to react with Mg (formed by decomposition of MgH_2) and form Al_3Mg_2 and $Mg_{17}Al_{12}$ by the following reactions:

$$3Al + 2Mg \rightarrow Al_3Mg_2 \quad (9)$$

$$12Al + 17Mg \rightarrow Mg_{17}Al_{12}. \quad (10)$$

Liu et al. [12] reported that when the temperature is increased to 633 K, a large amount of hydrogen has been released and two new phases, $Mg_{17}Al_{12}$ and Mg, are formed while the preformed Al and Al_3Mg_2 disappear. Samples were easily ignited and combusted during treatment, making difficult the obtention of XRD patterns and leading to the formation of a strong peak of MgO and relatively weak peaks of other phases.

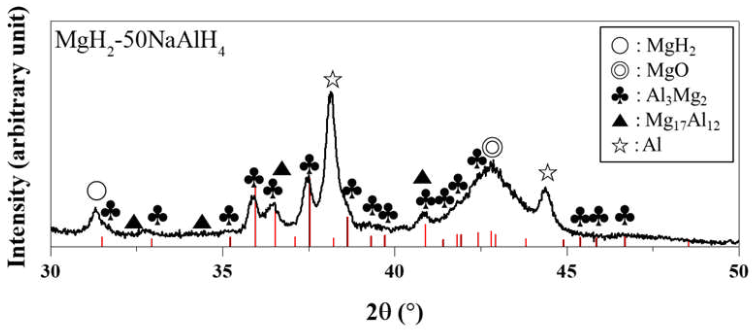

Figure 3. XRD pattern of MgH_2-50$NaAlH_4$ dehydrided after number of cycles, n, of 4 at 593 K.

Figure 4 shows the change of H_a versus time t curve at 593 K in 12 bar hydrogen with cycle number, n, for MgH_2-30$NaAlH_4$. The effective hydrogen-storage capacity is defined as the quantity of hydrogen absorbed for 60 min (wt% H). As n increases from one to two, the hydrogen-absorption rate for 1 min increases, and from n = 2 to n =4 the initial hydriding rate decreases. In a similar way, the effective hydrogen-storage capacity increases as n increases from one to two, and from n = 2 to n

Preprints (www.preprints.org) | NOT PEER-REVIEWED | Posted: 3 January 2024 doi:10.20944/preprints202401.0201.v1

= 4 the effective hydrogen-storage capacity decreases. The activation is considered to have been completed after n = 2. At n = 2, MgH_2-30$NaAlH_4$ absorbs 4.09 wt% H for 1 min, 7.17 wt% H for 10 min, and 7.42 wt% H for 60 min.

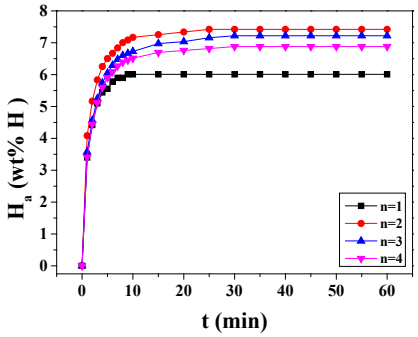

Figure 4. Change in quantity of absorbed hydrogen (H_a) versus time t curve at 593 K in 12 bar hydrogen with cycle number, n, for MgH_2-30$NaAlH_4$.

The change of H_r versus t curve at 593 K in 1.0 bar hydrogen with n for MgH_2-30$NaAlH_4$ is shown in Figure 5. As the number of cycles (n) increases from one to four, the hydrogen-release rate for 1 min decreases. The hydrogen-release rate for 1 min at n = 1 and n = 2 are very similar. The quantity of hydrogen released for 60 min increases as n increases from one to two, and from n = 2 to n =4 the quantity of hydrogen released for 60 min decreases. At n = 2, MgH_2-30$NaAlH_4$ releases 1.31 wt% H for 1 min, 4.95 wt% H for 10 min, and 7.34 wt% H for 60 min.

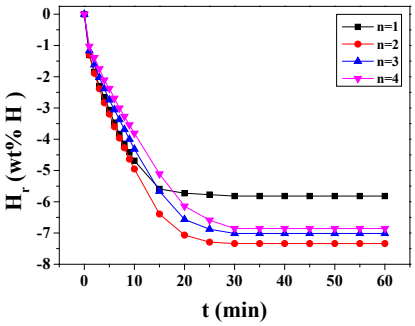

Figure 5. Change in quantity of released hydrogen (H_r) versus t curve at 593 K in 1.0 bar hydrogen with cycle number, n, for MgH_2-30$NaAlH_4$.

During hydrogen absorption (Figure 3) and release (Figure 4), the reactions (5) and (6) are believed to occur.

Figure 6 shows changes in H_a versus time t curve at 593 K in 12 bar hydrogen and H_r versus t curve at 593 K in 1.0 bar hydrogen with cycle number, n, for MgH_2-30$NaAlH_4$. The curves show that activation is completed after n = 2, showing the highest hydrogen-absorption rate, the highest hydrogen-release rate, the largest effective hydrogen-storage capacity, and the largest quantity of hydrogen released for 60 min.

Preprints (www.preprints.org) | NOT PEER-REVIEWED | Posted: 3 January 2024 doi:10.20944/preprints202401.0201.v1

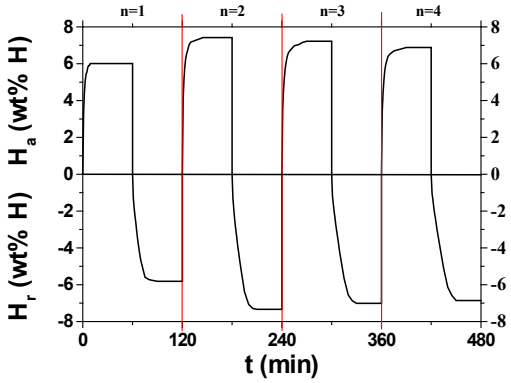

Figure 6. Changes in H_a versus t curve at 593 K in 12 bar hydrogen and H_r versus t curve at 593 K in 1.0 bar hydrogen with cycle number, n, for MgH_2-30$NaAlH_4$.

The H_a versus t curves in 12 bar hydrogen at 593 K or 623 K at n = 1 and n = 2 for MgH_2-50$NaAlH_4$ are shown in Figure 7. Because the hydrogen-absorption rate was low, experiments were performed several times. Even though the samples were handled in an Ar atmosphere, the samples were ignited and combusted partly, leading to low hydrogen-absorption rates and low effective hydrogen storage capacities. For n = 1 at 593 K, the MgH_2-50$NaAlH_4$ sample does not absorb hydrogen. For n = 2 at 623 K, the MgH_2-50$NaAlH_4$ sample does not absorb hydrogen either, probably because the difference between the applied hydrogen pressure (12 bar) and the equilibrium plateau pressure at 623 K (6.38 bar [13]) of the Mg-H system is small. At n = 2, the MgH_2-50$NaAlH_4$ sample absorbs 0.99 wt% H for 1 min, 1.36 wt% H for 10 min, and 3.19 wt% H for 60 min at 593 K.

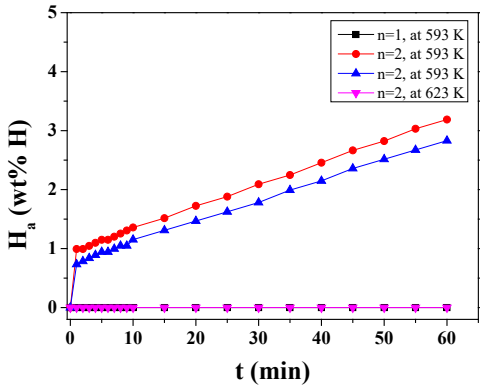

Figure 7. H_a versus t curves in 12 bar hydrogen at 593 K or 623 K at n = 1 and n = 2 for MgH_2-50$NaAlH_4$.

Figure 8 shows the H_r versus t curves in 1.0 bar hydrogen at 593 K or 623 K at n = 1 ~ 4 for MgH_2-50$NaAlH_4$. Hydrogen-release rates are low and the quantities of hydrogen released for 60 min are small. As n increases, the initial hydrogen-release rate and the quantity of hydrogen released for 60 min increase slightly. At n = 2, the MgH_2-50$NaAlH_4$ sample releases 1.03 wt% H for 5 min and 1.29 wt% H for 60 min at 593 K. When the temperature increases from 593 K to 623 K, the initial hydrogen-release rate and the quantity of hydrogen released for 60 min increase slightly. Partial ignition and combustion in the samples led to low initial hydrogen-release rates and small quantities of hydrogen released for 60 min.

Preprints (www.preprints.org) | NOT PEER-REVIEWED | Posted: 3 January 2024 doi:10.20944/preprints202401.0201.v1

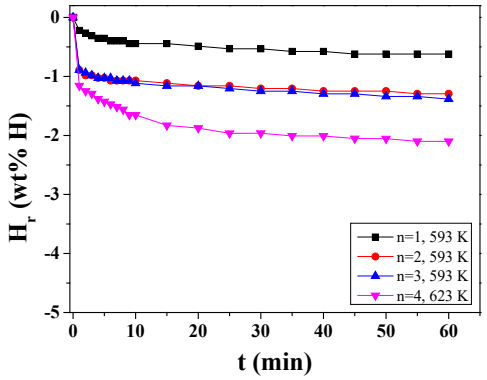

Figure 8. H_r versus t curves in 1.0 bar hydrogen at 593 K or 623 K at n = 1 ~ 4 for MgH_2-50$NaAlH_4$.

H_a versus t curves in 12 bar hydrogen at 593 K for activated MgH_2-30$NaAlH_4$, MgH_2-2Ni-10$NaAlH_4$ after RMM, activated Mg-10Fe_2O_3 [14,15], activated Mg-10TaF_5 [16,17], and activated Mg-10VCl_3 [18] are shown in Figure 9. The Mg-10Fe_2O_3 [14,15], Mg-10TaF_5 [16,17], and Mg-10VCl_3 [18] samples were also prepared by RMM under the conditions similar to those for preparing MgH_2-30$NaAlH_4$, MgH_2-2Ni-10$NaAlH_4$. MgH_2-2Ni-10$NaAlH_4$ did not require activation after reactive mechanical milling (RMM). The H_a versus t curve of MgH_2-2Ni-10$NaAlH_4$ after RMM is used for comparison with the H_a versus t curves of other activated samples. Activated MgH_2-30$NaAlH_4$ has the highest hydrogen-absorption rate for 2.5 min, followed in order by MgH_2-2Ni-10$NaAlH_4$ after RMM, activated Mg-10VCl_3, activated Mg-10TaF_5, and activated Mg-10Fe_2O_3. Activated MgH_2-30$NaAlH_4$ has the highest effective hydrogen-storage capacity, followed in order by activated Mg-10VCl_3, MgH_2-2Ni-10$NaAlH_4$ after RMM, activated Mg-10Fe_2O_3, and activated Mg-10TaF_5. MgH_2-30$NaAlH_4$ has much higher hydrogen-absorption rate for 2.5 min (2.20 wt% H/min) and much larger effective hydrogen-storage capacity (7.42 wt% H) than the other samples.

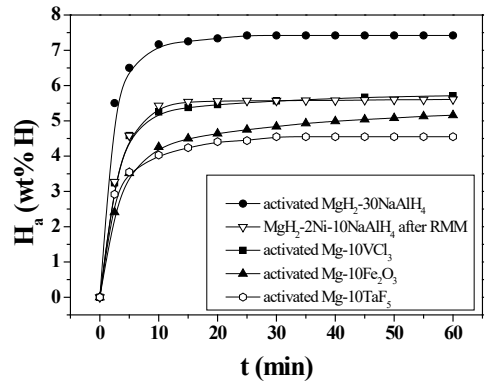

Figure 9. H_a versus t curves in 12 bar hydrogen at 593 K for activated MgH_2-30$NaAlH_4$, MgH_2-2Ni-10$NaAlH_4$ after RMM, activated Mg-10Fe_2O_3, activated Mg-10TaF_5, and activated Mg-10VCl_3.

Figure 10 shows H_r versus t curves in 1.0 bar hydrogen at 593 K for activated MgH_2-30$NaAlH_4$, MgH_2-2Ni-10$NaAlH_4$ after RMM, activated Mg-10Fe_2O_3, activated Mg-10TaF_5, and activated Mg-10VCl_3. Activated MgH_2-30$NaAlH_4$ has the highest hydrogen-release rate for 2.5 min, followed in order by activated Mg-10VCl_3, activated Mg-10TaF_5, MgH_2-2Ni-10$NaAlH_4$ after RMM, and activated Mg-10Fe_2O_3. Activated MgH_2-30$NaAlH_4$ has the largest quantity of hydrogen released for 60 min, followed in order by activated Mg-10VCl_3, MgH_2-2Ni-10$NaAlH_4$ after RMM, activated Mg-10TaF_5, and activated Mg-10Fe_2O_3, and activated. MgH_2-30$NaAlH_4$ has much higher hydrogen-release rate for 2.5 min (0.86 wt%/min) and much larger quantity of hydrogen released for 60 min (7.34 wt% H) than the other samples.

Preprints (www.preprints.org) | NOT PEER-REVIEWED | Posted: 3 January 2024 doi:10.20944/preprints202401.0201.v1

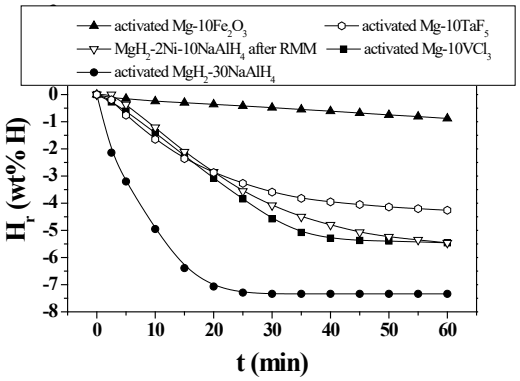

Figure 10. H_r versus t curves in 1.0 bar hydrogen at 593 K for activated MgH_2-30$NaAlH_4$, MgH_2-2Ni-10$NaAlH_4$ after RMM, activated Mg-10Fe_2O_3, activated Mg-10TaF_5, and activated Mg-10VCl_3.

4. Discussion

From the results of Fig. 2, it is believed that for the $NaAlH_4$, the reaction (1) [decomposition of $NaAlH_4$] begins to occur at 438 K and the reaction (2) [decomposition of Na_3AlH_6] begins to occur at 495 K. For the MgH_2-10$NaAlH_4$ sample, it is believed that the reaction (4) occurs between the point 1 (508 K) and the point 2 (525 K), the reactions (5) and (6) begins to occur after the point 3 (550 K), and then the reaction (7) and the reaction (8) occur consecutively. For the MgH_2-30$NaAlH_4$ sample, it is believed that the reaction (4) occurs between the point 1 (480 K) and the point 2 (541 K), the reactions (5) and (6) begins to occur after the point 3 (562 K), and then the reaction (7) and the reaction (8) occur consecutively. The reaction (4) for the MgH_2-30$NaAlH_4$ begins to occur at 28 K lower temperature than that for the MgH_2-10$NaAlH_4$.

Samples were easily ignited and combusted during treatment, making difficult the obtention of XRD patterns and leading to the formation of a strong peak of MgO and relatively weak peaks of other phases. Liu et al. [12] reported that when the temperature is increased to 633 K, the preformed Al and Al_3Mg_2 disappear. In Fig. 3 (the XRD pattern of MgH_2-50$NaAlH_4$ dehydrided after number of cycles, n, of 4 at 593 K), the Al_3Mg_2 phase is observed. The dehydriding temperature (593 K) lower than that in the work of Liu et al. [12] is believed to have led to this result.

As the content of $NaAlH_4$ in the sample increases, the temperature at the highest peak in the ratio of increase in H_r to increase in T, dH_r/dT, versus T curve decreases. The higher content of $NaAlH_4$ is believed to have made effects of reactive mechanical milling stronger. However, too much content of $NaAlH_4$ (as in MgH_2-50$NaAlH_4$) leads to worse hydrogen-storage properties (hydrogen-absorption rate, hydrogen-release rate, and hydrogen-storage capacity).

RMM creates defects and cracks. The propagation of cracks makes the particles finer. Defects can be used as the sites active for nucleation. Decrease in particle size reduces the diffusion distance of hydrogen atoms. The added materials and formed phases are believed to make the effects of RMM stronger. The expansion of lattice due to hydrogen absorption and the contraction of lattice due to hydrogen release causes the effects similar to those of RMM. However, the effects of lattice expansion and contraction will be weaker than those of RMM. The MgH_2-30$NaAlH_4$ sample has a higher hydrogen-absorption rate for 2.5 min, a larger effective hydrogen-storage capacity, a higher hydrogen-release rate for 2.5 min, and a larger quantity of hydrogen released for 60 min than the other samples, showing that the effects of RMM and hydrogen absorption-release cycling are stronger in the MgH_2-30$NaAlH_4$ sample, compared with those for the other samples. Reportedly, nucleation can be facilitated by creating active nucleation sites by mechanical treatment and/or alloying with additives [19]; the diffusion distance of hydrogen can also be decreased by the mechanical treatment and/or alloying of Mg with additives, thereby reducing the magnesium particle size [20]; in addition, the hydrogen mobility can be improved by additives that create microscopic paths of hydrogen [20]; a rough surface of magnesium particles having many cracks and defects is thus considered more advantageous for hydrogen absorption [21].

In our future work, milled $NaAlH_4$ will be prepared by reactive mechanical milling. The quantity of released hydrogen (H_r) versus temperature T curve and the ratio of increase in H_r to increase in T, dH_r/dT, versus T curve for the milled $NaAlH_4$ will be obtained and studied in detail. Behaviors of the milled $NaAlH_4$, which are different from those of $NaAlH_4$, are expected.

As shown in Figures 9 and 10, addition effects of $NaAlH_4$, oxide, halides, or fluoride to MgH_2 or Mg are different. Which kinds of properties such as physical properties (hardness, toughness, surface area, and microstructure, etc.) and chemical properties affect the hydrogen-storage properties will be investigated.

5. Conclusions

In this work, milled MgH_2, $NaAlH_4$, MgH_2–10$NaAlH_4$ (with a composition of 90 wt% MgH_2 + 10 wt% $NaAlH_4$), MgH_2–30$NaAlH_4$ (70 wt% MgH_2 + 30 wt% $NaAlH_4$), MgH_2–50$NaAlH_4$ (50 wt% MgH_2 + 50 wt% $NaAlH_4$), and MgH_2–2Ni-10$NaAlH_4$ (88 wt% MgH_2 + 2 wt% Ni + 10wt% $NaAlH_4$) samples were prepared by reactive mechanical milling (RMM). As the content of $NaAlH_4$ in the sample increased, the temperature at the highest peak in the ratio of increase in H_r to increase in T, dH_r/dT, versus T curve decreased. The higher content of $NaAlH_4$ is believed to have made effects of reactive mechanical milling stronger. MgH_2-50$NaAlH_4$ dehydrided after four cycles contained Al, MgO, Al_3Mg_2, MgH_2, and $Mg_{17}Al_{12}$. Hydriding in 12 bar hydrogen and dehydriding in 1.0 bar hydrogen at 593 K of MgH_2-30$NaAlH_4$ are performed by the reversible reactions $MgH_2 \Leftrightarrow Mg + H_2$ and $17MgH_2 + 12Al \Leftrightarrow Mg_{17}Al_{12} + 17H_2$. Activation of MgH_2–30$NaAlH_4$ was completed after two hydrogen absorption-release cycles. MgH_2–30$NaAlH_4$ was the best Mg-based composite among Mg-based alloys in which an oxide, a halide, a fluoride, or a complex hydride was added, with a high hydrogen-absorption rate for 2.5 min (2.20 wt% H/min) and a large effective hydrogen-storage capacity (7.42 wt% H).

Author Contributions: Conceptualization, Kwak, Y.J.; Song, M.Y.; Lee, K.-T.; methodology, Kwak, Y.J.; Song, M.Y.; Lee, K.-T.; formal analysis, Kwak, Y.J.; Song, M.Y.; Lee, K.-T.; investigation, Kwak, Y.J.; Song, M.Y.; Lee, K.-T.; data curation, Kwak, Y.J.; writing—original draft preparation, Kwak, Y.J.; Song, M.Y.; writing—review and editing—Kwak, Y.J.; Song, M.Y.; Lee, K.-T.; project administration, Kwak, Y.J.; Lee, K.-T.; funding acquisition, Kwak, Y.J.; All authors have read and agreed to the published version of the manuscript.

Funding: This work was supported by the National Research Foundation of Korea (NRF) grant funded by the Korean government (MSIT) (No. 2021R1C1C2009103). This work was supported by Korea Institute of Energy Technology Evaluation and Planning (KETEP) grant funded by the Korea government (MOTIE) (20213030040110).

Data Availability Statement: The *data* that support the findings of this study are *available* on *request* from the *corresponding author*, [M Y S].

Conflicts of Interest: The authors declare no conflict of interest.

References

1. Reilly, J.J.; Wiswall, R.H. Reaction of hydrogen with alloys of magnesium and nickel and the formation of Mg_2NiH_4. *Inorg. Chem.* **1968**, *7*, 2254–2256. https://doi.org/10.1021/ic50069a016.
2. Karty, A.; Genossar, J.G.; Rudman, P.S. Hydriding and dehydriding kinetics of Mg in a Mg/Mg_2Cu eutectic alloy: Pressure sweep method. *J. Appl. Physics* **1979**, *50*, 7200–7209. https://doi.org/10.1063/1.325832.
3. Akiba, E.; Nomura, K.; Ono, S.; Suda, S. Kinetics of the reaction between Mg-Ni alloys and H_2. *Int J. Hydrogen Energy* **1982**, *7*, 787–791. https://doi.org/10.1016/0360-3199(82)90069-6.
4. Bobet, J.-L.; Akiba, E.; Nakamura, Y.; Darriet, B. Study of Mg–M (M = Co, Ni and Fe) mixture elaborated by reactive mechanical alloying-hydrogen sorption properties. *Int. J. Hydrogen Energy* **2000**, *25*, 987–996. https://doi.org/10.1016/S0360-3199(00)00082-3.
5. Huot, J.; Ravnsbæk, D.B.; Zhang, J.; Cuevas, F.; Latroche, M.; Jensen, T.R. Mechanochemical synthesis of hydrogen storage materials. *Prog. Mater. Sci.* **2013**, *58*, 30–75. https://doi.org/10.1016/j.pmatsci.2012.07.001.
6. Song, M.Y.; Ahn, D.S.; Kwon, I.H.; Ahn, H.J. Development of Hydrogen storage Alloys by Mechanical Alloying Mg with Fe and Co. *Met. Mater. Int.* **1999**, *5*, 485–490. https://doi.org/10.1007/BF03026163.
7. Ali, N.A.; Ismail, M. Advanced hydrogen storage of the Mg–Na–Al system: A review. *J. Magnesium Alloys* **2021**, *9*, 1111–1122. https://doi.org/10.1016/j.jma.2021.03.031.

8. Plerdsranoy, P.; Meethom, S.; Utke, R. Dehydrogenation kinetics, reversibility, and reaction mechanisms of reversible hydrogen storage material based on nanoconfined MgH_2−$NaAlH_4$. *J. Phys. Chem. Solids* **2015**, *87*, 16–22. https://doi.org/10.1016/j.jpcs.2015.07.018.
9. Rafi-ud-din; Xuanhui, Q.; Ping, L.; Zhang, L.; Ahmad, M.; Iqbal, M.Z.; Rafique, M.Y.; Farooq, M.H. Enhanced hydrogen storage performance for MgH_2–$NaAlH_4$ system—The effects of stoichiometry and Nb_2O_5 nanoparticles on cycling behaviour. *RSC Adv.* **2012**, *2*, 4891–4903. https://doi.org/10.1039/C2RA20518A.
10. Ismail, M.; Zhao, Y.; Yu, X.B.; Mao, J.F.; Dou, S.X. The hydrogen storage properties and reaction mechanism of the MgH_2–$NaAlH_4$ composite system. *Int. J. Hydrogen Energy* **2011**, *36*, 9045–9050. https://doi.org/10.1016/j.ijhydene.2011.04.132.
11. Bendyna, J.K.; Dyjak, S.; Notten, P.H.L. The influence of ball-milling time on the dehydrogenation properties of the $NaAlH_4$–MgH_2 composite. *Int. J. Hydrogen Energy* **2015**, *40*, 4200–4206. https://doi.org/10.1016/j.ijhydene.2015.01.026.
12. Liu, H.; Wang, X.; Liu, Y.; Dong, Z.; Ge, H.; Li, S.; Yan, M. Hydrogen Desorption Properties of the MgH_2–AlH_3 Composites. *J. Phys. Chem.C* **2014**, *118*, 37–45. https://doi.org/10.1021/jp407018w.
13. Stampfer, J.F.; Molley, C.E.; Suttle, J.F. The Magnesium-Hydrogen System1-3. *J. Am. Chem. Soc.* **1960**, *82*, 3504–3508. https://doi.org/10.1021/ja01499a006.
14. Song, M.Y.; Kwon, I.H.; Kwon, S.N.; Park, C.G.; Hong, S.-H.; Bae, J.-S.; Mumm, D.R. Hydrogen-storage properties of Mg–oxide alloys prepared by reactive mechanical grinding. *J. Alloys Compd.* **2006**, *415*, 266–270. https://doi.org/10.1016/j.jallcom.2005.08.002.
15. Song, M.Y.; Kwon, S.N.; Park, H.R. Pressure-Composition Isotherms and Cycling Properties of Mg-xFe_2O_3-yNi Alloys. *Korean J. Met. Mater.* **2013**, *51*, 455–460. https://kiss.kstudy.com/Detail/Ar?key=3142396.
16. Kwak, Y.J.; Lee, S.H.; Park, H.R.; Song, M.Y. Review Paper : Hydriding and Dehydriding Reactions of Mg-xTaF_5 (x=0, 5, and 10) Prepared via Reactive Mechanical Grinding. *Korean J. Met. Mater.* **2014**, *52*, 957–962. https://kiss.kstudy.com/Detail/Ar?key=3272039.
17. Kwak, Y.J.; Lee, S.H.; Park, H.R.; Song, M.Y. Hydrogen Storage Characteristics of Mg, Mg-5TaF_5, and Mg-5NbF_5 Prepared via Grinding in a Hydrogen Atmosphere. *J. Nanoscience and Nanotechnology* **2016**, *16*, 10508–10514. https://doi.org/10.1166/jnn.2016.13185.
18. Song, M.Y.; Lee, S.H.; Mumm, D.R. Fe_2O_3, MnO, and VCl_3-added Mg composites by reactioninvolving grinding processing for hydrogen storage. *J. Cer. Proc. Res* **2018**, 19(3), 211-217. https://doi.org/10.36410/JCPR.2018.19.3.211-217.
19. Hjort, P.; Krozer, A.; Kasemo, B. Hydrogen sorption kinetics in partly oxidized Mg films. *J. Alloys Comp.* **1996**, 237(1-2), 74-80. https://doi.org/10.1016/0925-8388(95)02165-5.
20. Zaluska, A.; Zaluski, L.; Ström-Olsen, J.O. Nanocrystalline magnesium for hydrogen storage. *J. Alloys Comp.* **1999**, *288*, 217–225. https://doi.org/10.1016/S0925-8388(99)00073-0.
21. Vigeholm, B.; Kjoller, J.; Larsen, B.; Pedersen, A.S. Formation and decomposition of magnesium hydride. *J. Less-Common Met.* **1983**, 89(1), 135-144. https://doi.org/10.1016/0022-5088(83)90259-X.